

# KLF4 Coordinates Corneal Epithelial Apical-Basal Polarity and Plane of Cell Division and Is Downregulated in Ocular Surface Squamous Neoplasia

Anil Tiwari,<sup>1</sup> Sudha Swamynathan,<sup>1</sup> Vishal Jhanji,<sup>1</sup> and Shivalingappa K. Swamynathan<sup>1-4</sup>

<sup>1</sup>Department of Ophthalmology, University of Pittsburgh School of Medicine, Pittsburgh, Pennsylvania, United States

<sup>2</sup>Department of Cell Biology, University of Pittsburgh School of Medicine, Pittsburgh, Pennsylvania, United States

<sup>3</sup>Fox Center for Vision Restoration, University of Pittsburgh School of Medicine, Pittsburgh, Pennsylvania, United States

<sup>4</sup>McGowan Institute of Regenerative Medicine, University of Pittsburgh, Pennsylvania, United States

Correspondence: Shivalingappa K. Swamynathan, University of Pittsburgh School of Medicine, 203 Lothrop Street, Room 1025, Pittsburgh, PA 15213, USA; [swamynathansk@upmc.edu](mailto:swamynathansk@upmc.edu).

Received: January 16, 2020

Accepted: March 5, 2020

Published: May 12, 2020

Citation: Tiwari A, Swamynathan S, Jhanji V, Swamynathan SK. KLF4 coordinates corneal epithelial apical-basal polarity and plane of cell division and is downregulated in ocular surface squamous neoplasia. *Invest Ophthalmol Vis Sci.* 2020;61(5):15. <https://doi.org/10.1167/iov.61.5.15>

**PURPOSE.** Previously, we demonstrated that Krüppel-like factor 4 (KLF4) promotes corneal epithelial (CE) homeostasis by suppressing epithelial-mesenchymal transition (EMT) and TGF- $\beta$  signaling. As TGF- $\beta$  affects epithelial apicobasal polarity (ABP) and plane of division, we investigated the role of KLF4 in these processes.

**METHODS.** *Klf4* was ablated in adult ternary transgenic *Klf4 $\Delta/\Delta$ CE* (*Klf4<sup>LoxP/LoxP</sup>/Krt12<sup>rtTA/rtTA</sup>/Tet-O-Cre*) mouse CE using doxycycline chow. ABP and plane of division markers' expression in *Klf4 $\Delta/\Delta$ CE* and human ocular surface squamous neoplasia (OSSN) tissues relative to controls was evaluated by quantitative PCR, immunoblots, and/or immunofluorescent staining.

**RESULTS.** *Klf4 $\Delta/\Delta$ CE* CE cells displayed downregulation of apical Pals1 and Crumbs1, apicolateral Par3, and basolateral Scribble, as well as upregulation of Rho family GTPase Cdc42, suggesting disruption of ABP. Phalloidin staining revealed that the *Klf4 $\Delta/\Delta$ CE* CE actin cytoskeleton is disrupted. *Klf4 $\Delta/\Delta$ CE* cells favored vertical plane of division within 67.5° to 90° of the CE basement membrane (39% and 47% of the dividing cells relative to 23% and 26% in the control based on phospho-histone-H3 and survivin, respectively), resulting in more dividing cells within the *Klf4 $\Delta/\Delta$ CE* CE as reported previously. *KLF4* was downregulated in human OSSN tissues that displayed EMT and downregulation of PAR3, PALS1, and SCRIB, consistent with a protective role for KLF4.

**CONCLUSIONS.** By demonstrating that *Klf4* ablation affects CE expression of ABP markers and Cdc42, cytoskeletal actin organization, and the plane of cell division and that KLF4 is downregulated in OSSN tissues that display EMT and lack ABP, these results elucidate the key integrative role of KLF4 in coordinating CE cell polarity and plane of division, loss of which results in OSSN.

Keywords: corneal epithelium, KLF4, apicobasal polarity, plane of division, EMT, OSSN

The corneal epithelium (CE), the anterior-most part of the eye that provides the transparent barrier function, is a self-renewing stratified squamous tissue comprising basal proliferating cells that serve as a source for the differentiating suprabasal and terminally differentiated superficial cells, which are eventually sloughed off.<sup>1</sup> Cellular polarity—polarized distribution of protein complexes involved in cell-cell and cell-matrix interactions—is a fundamental determinant of epithelial cell properties.<sup>2-4</sup> Epithelial cell polarity manifests as apicobasal polarity (ABP; polarization along the apicobasal axis that facilitates apical barrier formation and basal adhesion to basement membrane) and planar cell polarity (PCP; polarization along the orthogonal axis within the plane of the epithelium). Establishment and maintenance of correct cellular polarity are essential for all epithelial cells, including the CE for their specialized cellular functions and homeostasis.<sup>3</sup> A proper balance between CE cell proliferation and differentiation is essential for its homeostasis.<sup>5</sup>

Disruption of this balance results in severe visual impairments, including epithelial erosion, dry eye, corneal fibrosis, and rare ocular tumors such as ocular surface squamous neoplasia (OSSN).<sup>6</sup> Although the core PCP protein Vangl2 is reported to influence the CE cell migration and ABP organization,<sup>7,8</sup> little else is known about the functions of ABP in CE. While studies in other stratified tissues such as the skin suggest that ABP regulates the vectorial distribution of information from basal to apical cells,<sup>2</sup> the molecular events that coordinate directionality and transmission of such information in the CE cells are poorly understood.

Epithelial ABP is established by the differential localization of three major membrane-associated protein complexes: the apical Crumbs complex comprising Crumbs1 (Crb), Pals1, and Patj; apicolateral Par complex consisting of Par6, Par3, and atypical PKC; and the basolateral Scribble complex composed of Scribble, Dlg, and Lgl.<sup>3,9</sup> Components of Par complex interact with other apical polarity regulating factors

such as Pals1,<sup>10</sup> which acts as a scaffold between PatJ and Crb to form a Crb/Pals1/PatJ complex localized at the tight junctions.<sup>11</sup> ABP complex components also interact with the small GTPases Rho/Rac/Cdc42 that in turn help maintain F-actin cytoskeleton, providing structural stability to epithelial tissues.<sup>9,12,13</sup> Besides maintaining ABP and cytoskeletal architecture, cell polarity proteins also facilitate directional spindle assembly and asymmetric cell divisions in stem and transiently amplifying cells, which result in a daughter cell that undergoes differentiation while the other retains the renewal potential.<sup>14,15</sup> Although it is widely recognized that the asymmetric localization of multiprotein complexes that demarcate the apical, lateral, and basal aspects of an epithelial cell is evolutionarily conserved, how their expression is coordinated remains relatively understudied.

Previous studies from our laboratory and others identified the Krüppel-like factor 4 (Klf4), one of the most abundantly expressed transcription factors in the cornea, as a major determinant of CE properties.<sup>16,17</sup> Corneal Klf4-target genes collectively promote CE structural stability and barrier functions while suppressing epithelial-mesenchymal transition (EMT) and TGF- $\beta$  signaling.<sup>16,18–23</sup> Although Klf4 is known to influence the intestinal epithelial cell ABP,<sup>24</sup> its involvement in regulating the core ABP determinants is unexplored in stratified tissues such as the CE. Given that (1) Klf4 is abundantly expressed in the cornea where it upregulates the expression of tight and adherence junction components that play a key role in CE ABP,<sup>21</sup> (2) Klf4 ablation results in EMT and increased TGF- $\beta$  signaling commonly associated with compromised ABP and epithelial tumors,<sup>22,23</sup> (3) TGF- $\beta$ -induced EMT is invariably associated with a loss of ABP,<sup>25</sup> and (4) decreased expression or mutations in Klf4 are commonly associated with tumors<sup>26,27</sup> that display loss of core polarity components and altered plane of cell division,<sup>28</sup> we predicted that Klf4 contributes to CE homeostasis by coordinating CE cell ABP and plane of division. Data presented in this report reveal that spatiotemporally regulated ablation of Klf4 in the adult mouse CE affects (1) the expression of a functionally related subset of core ABP determinants Pals1, Crumbs1, Par3, and Scribble; (2) expression of Rho family GTPase Cdc42; (3) cytoskeletal F-actin organization; and (4) the plane of cell division, elucidating the key integrative role of Klf4 in coordinating CE cellular ABP and plane of division. Moreover, KLF4 was downregulated in human OSSN tissues that displayed signs of EMT and loss of ABP, suggesting that mutations or altered expression of KLF4 are a potential causative factor for human OSSN.

## MATERIALS AND METHODS

### Animals

All experiments were performed in accordance with the University of Pittsburgh Institutional Animal Care and Use Committee (IACUC protocol 17019882, titled “Role of Krüppel-Like Factors in the Ocular Surface”; PI: Swamyathan) and the ARVO Statement on the Use of Animals in Ophthalmic and Vision Research. All studies were conducted with 8- to 10-week-old mice, housed at the University of Pittsburgh animal facility with a 12-hour dark/light cycle. Ternary transgenic *Klf4 $\Delta/\Delta$ CE* (*Klf4<sup>LoxP/LoxP</sup>/Krt12<sup>rTA/rTA</sup>/Tet-O-Cre*) mice were derived as described previously<sup>19</sup> by natural interbreeding between *Klf4<sup>LoxP/LoxP</sup>* (a kind gift of Dr. Klaus Kaestner, University of Pennsylvania)<sup>29</sup> and binary

transgenic *Krt12<sup>rTA/rTA</sup>/Tet-O-Cre* mice (a kind gift of Dr. Winston Kao, University of Cincinnati).<sup>30</sup> Spatiotemporal ablation of *Klf4* in adult mouse CE was achieved by feeding 8- to 10-week-old *Klf4 $\Delta/\Delta$ CE* mice with doxycycline (Dox) chow (cat. S3888, 200 mg Dox/kg chow; BioServ, Flemington, NJ, USA) for at least a month as earlier.<sup>19</sup> As Krt12 is expressed in a monoallelic manner,<sup>31</sup> we maintained *Krt12-rTA* in a homozygous condition to ensure its uniform expression throughout the CE. Age- and sex-matched littermates with the same genotype (*Klf4<sup>LoxP/LoxP</sup>/Krt12<sup>rTA/rTA</sup>/Tet-O-Cre*) fed with regular chow (without doxycycline) served as control.

### Collection and Processing of Human Normal Corneas and OSSN Samples

Normal human corneas were sourced from donor corneal tissues rejected for transplants, following the procedures approved by the University of Pittsburgh Committee for Oversight of Research and Clinical Training Involving Deceaseds (CORID ID 889, titled “Krüppel-Like Factors in the Corneal Epithelium”; PI: Swamyathan). Human OSSN samples were collected following the institutional review board-approved protocol (PRO-18100052, titled “Ocular Surface Squamous Neoplasia”; PI: Jhanji).

### Total RNA Isolation and Quantitative RT-PCR

Total RNA was isolated from dissected mouse corneas or OSSN tissues using EZ-10 spin column total RNA mini-prep kit (Bio Basic, Inc., Amherst, NY, USA). Isolated RNA (500 ng) was used for cDNA synthesis with mouse Maloney leukemia virus reverse transcriptase (Promega, Madison, WI, USA). SYBR Green quantitative RT-PCR (RT-qPCR) gene expression assays were performed in triplicate in an ABI StepOne Plus thermocycler using appropriate endogenous controls (Applied Biosystems, Foster City, CA, USA). The sequence of oligonucleotide primers used for RT-qPCR (synthesized by Integrated DNA Technologies, Inc., Coralville, IA) is presented in Supplementary Table S2.

### Immunoblots

Antibodies used in study are listed in Supplementary Table S3. Dissected *Klf4 $\Delta/\Delta$ CE* or control corneas were homogenized in urea buffer (8.0 M urea, 0.8% Triton X-100, 0.2% SDS, 3%  $\beta$ -mercaptoethanol, and protease inhibitors) and clarified by centrifugation. Then, 20  $\mu$ g total protein in the supernatant was separated on 4% to 12% gradient polyacrylamide gels using 3-(N-morpholino) propanesulfonic acid/2-(N-morpholino) ethanesulfonic acid buffer and blotted onto polyvinylidene fluoride membranes of 0.45  $\mu$ m pore size (Invitrogen, Carlsbad, CA, USA). The membranes were blocked with Pierce protein-free (PBS) blocking buffer (Pierce, Rockford, IL, USA) for 1 hour at room temperature, incubated overnight at 4°C with appropriate dilution of primary antibody prepared in a 1:1 mixture of blocking buffer and PBS containing 0.2% Tween-20, washed thrice with PBS containing 0.1% Tween-20 (PBST) for 5 minutes each, incubated with fluorescently labeled secondary antibody (goat anti-rabbit IgG or donkey anti-goat IgG) for 1 hour at 23°C, and washed three times with PBST for 5 minutes each, followed by a wash with PBS to remove traces of Tween-20. Blots were scanned on an Odyssey scanner

(Li-Cor Biosciences, Lincoln, NE, USA) and densitometric measurements of the immunoreactive band intensities performed using ImageJ software (<http://imagej.nih.gov/ij/>; provided in the public domain by the National Institutes of Health, Bethesda, MD, USA).  $\beta$ -Actin was used as a loading control for normalizing the data.

### Immunofluorescent Staining

Eight-micrometer-thick sections from optimal cutting temperature compound (OCT)-embedded OSSN tissues, *Klf4* <sup>$\Delta/\Delta$ CE</sup>, or control eyeballs were fixed in buffered 4% paraformaldehyde for 10 minutes at 23°C, washed thrice for 5 minutes each with PBS (pH 7.4), permeabilized (0.1% Triton X-100 in PBS) when necessary followed by three washes of 5 minutes each with PBS, treated with glycine for 20 minutes, washed thrice with PBS, blocked (10% goat or donkey serum in PBS) for 1 hour at 23°C in a humidified chamber, washed twice with PBS for 5 minutes each, incubated with the appropriate dilution of the primary antibody for 2 hours at 23°C or overnight at 4°C, washed thrice with PBS for 5 minutes each, incubated with appropriate secondary antibody (Alexa Fluor 546-coupled goat anti-rabbit IgG, Alexa Fluor 488-coupled goat anti-mouse IgG or Alexa Fluor 488-coupled donkey anti-goat IgG; Molecular Probes, Carlsbad, CA, USA) at a 1:400 dilution for 1 hour at 23°C, washed thrice with PBST, counterstained with 4,6-diamidino-2-phenylindole (DAPI), mounted with Aqua-Poly/Mount (Polysciences, Warrington, PA, USA), and imaged using an Olympus IX81 microscope (Olympus America, Inc., Center Valley, PA). Actin cytoskeletal organization was visualized by staining with fluorescently tagged phalloidin (Molecular Probes, Carlsbad, CA). When these data were used to trace the CE cell boundaries for determining the plane of cell division, phalloidin stain intensity was empirically adjusted to variable extents during postprocessing using Fluoview software (Olympus America, Inc.).

### Analysis, Measurement, and Quantification of Mitotic Spindle Orientation

Cryosections from OCT-embedded control and *Klf4* <sup>$\Delta/\Delta$ CE</sup> eyeballs were immunofluorescently stained as described above with antisurvivin and anti-phospho-histone H3 (PH3) antibodies to identify the mitotic cells, as well as counterstained with DAPI, and the immunostaining pattern was used to determine the plane of division in the basal epithelial cells. Cells were taken into consideration only if both the daughter nuclei surrounding the survivin/PH3 immunostaining could be clearly identified. Distribution of the plane of division was quantified by analyzing four adjacent images from the central CE in four sections each from five different control and *Klf4* <sup>$\Delta/\Delta$ CE</sup> eyeballs. Mean counts were obtained in a blinded fashion from 75 and 93 nuclei that stained positive for PH3, as well as 171 and 342 nuclei that stained positive for survivin, respectively, from the control and *Klf4* <sup>$\Delta/\Delta$ CE</sup> CE. The angle of division was calculated by plotting a line passing through the centers of the two nuclei relative to the basement membrane. The angle of division is represented in 22.5° increments from 0° to 90°. Cell divisions positioned at 0° to 22.5° relative to the basement membrane were considered horizontal, those at 67.5° to 90° were considered verti-

cal, and the remaining oriented at 22.5° to 67.5° were considered oblique.

### Statistical Analysis

The number of samples used in each experiment is indicated in the corresponding figure legends. The results presented here are representative of at least three independent experiments and shown as mean  $\pm$  SEM. Statistical significance was tested by Student's t-test, with  $P \leq 0.05$  considered statistically significant.

## RESULTS

### Apicobasal Polarity Is Disrupted in *Klf4* <sup>$\Delta/\Delta$ CE</sup> CE

As reported previously,<sup>16,19,21,22</sup> CE-specific ablation of *Klf4* resulted in hyperplasia concurrent with downregulation of CE markers keratin 12 (Krt12), tight junction protein 1 (Tjp1), and E-cadherin, reminiscent of EMT (Supplementary Fig. S1). Given that (1) TJP1 colocalizes with Par3,<sup>32</sup> (2) EMT is associated with loss of epithelial ABP, and (3) loss of adhesion molecules such as E-cadherin and TJP1 impairs CE barrier function, which in turn is associated with altered localization of Par3 complex,<sup>18,32</sup> we hypothesized that the ablation of *Klf4* disrupts CE ABP. Consistent with that prediction, RT-qPCR revealed significant downregulation of *Par3*, *Pals1*, *Crumbs*, and *Scrib* transcripts in *Klf4* <sup>$\Delta/\Delta$ CE</sup> compared with the control CE (Fig. 1A). Corresponding decrease in Par3, Pals1, and Scrib protein expression in the *Klf4* <sup>$\Delta/\Delta$ CE</sup> corneas was confirmed by immunoblots (Fig. 1B). Immunofluorescent staining in the control CE revealed apicolateral cortical localization of Par3 and Pals1, apical localization of Crumbs, and basolateral expression of Scrib indicating proper apical-basal polarization (Fig. 1). In contrast, *Klf4* <sup>$\Delta/\Delta$ CE</sup> corneas displayed sharply decreased expression of Par3, Pals1, Crumbs1, and Scrib (Fig. 1C, Supplementary Fig. S2). Collectively, these results suggest that the CE-specific ablation of *Klf4* results in downregulation of ABP markers and that *Klf4* regulates the CE expression of a functionally related subset of proteins that play an important role in establishing and maintaining ABP.

### Cdc42 Expression and Cytoskeletal Actin Organization Is Disrupted in the *Klf4* <sup>$\Delta/\Delta$ CE</sup> CE

An array of signaling pathways participates in the regulation of ABP.<sup>33</sup> Among them, Rho GTPase pathway is prominent, being implicated in diverse events that depend on cellular polarity. The best characterized members of the Rho family—Cdc42, Rho, and Rac—play crucial roles in maintaining cellular structure and function by regulating the actin cytoskeletal organization.<sup>12,13,34,35</sup> Therefore, we examined if Rho GTPase expression is affected in *Klf4* <sup>$\Delta/\Delta$ CE</sup> CE concomitant with its disrupted ABP. We observed significantly increased levels of Cdc42 mRNA and protein in *Klf4* <sup>$\Delta/\Delta$ CE</sup> corneas compared with the control (Figs. 2A, 2B). Immunofluorescent stain further revealed strong cortical positioning of Cdc42 in both the control and the *Klf4* <sup>$\Delta/\Delta$ CE</sup> CE, with much more abundant expression in the *Klf4* <sup>$\Delta/\Delta$ CE</sup> cytoplasm (Fig. 2C). Although RhoA and RhoB transcripts were moderately upregulated in the *Klf4* <sup>$\Delta/\Delta$ CE</sup> corneas (Fig. 2A), a commensurate increase in the protein levels was not observed by immunoblot using antibody against RhoA/B/C in *Klf4* <sup>$\Delta/\Delta$ CE</sup> corneas (Fig. 2B). Consistently,

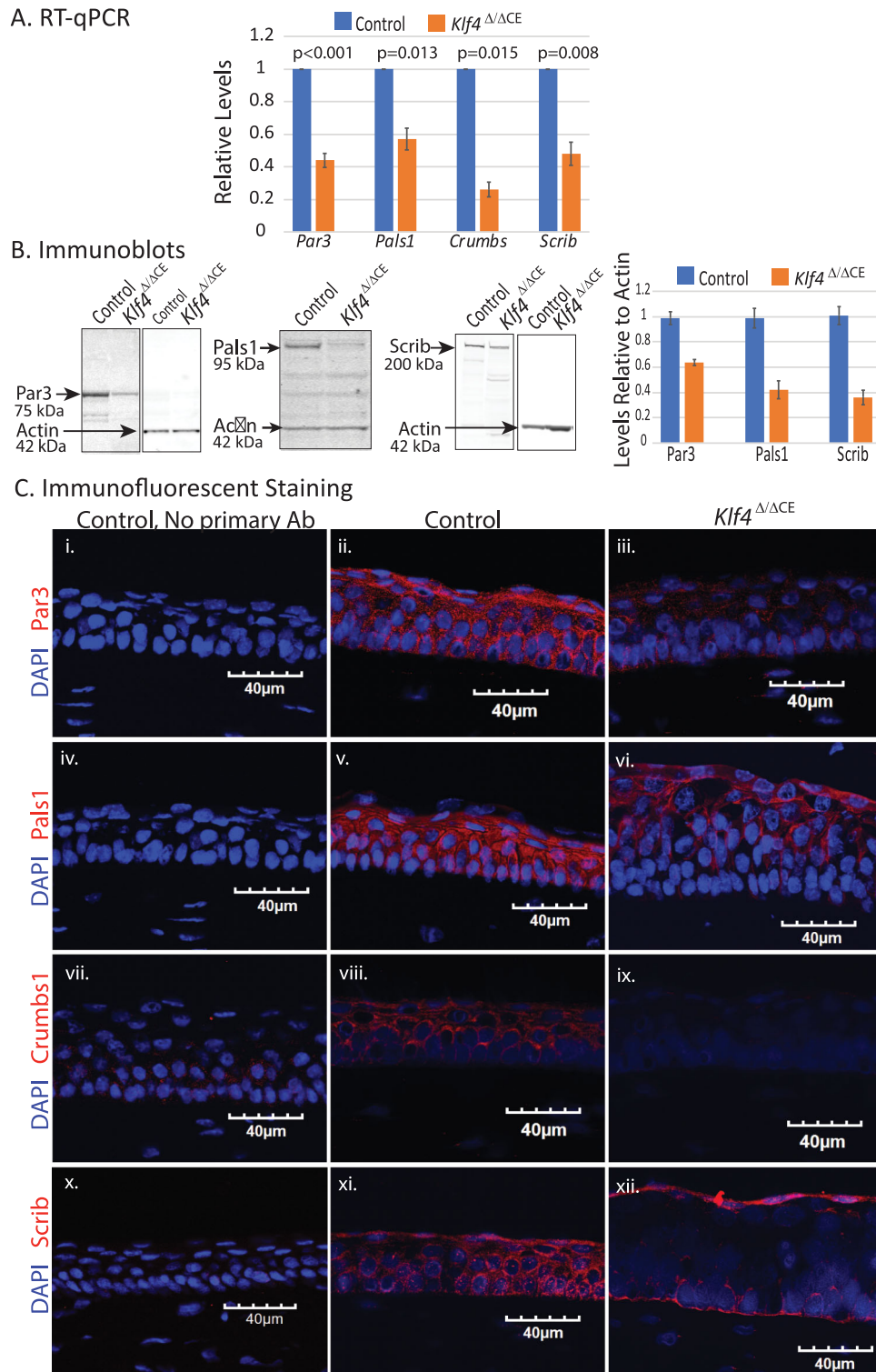


**FIGURE 1.** Apicobasal polarity is disrupted in *Klf4*<sup>Δ/ΔCE</sup> corneal epithelium. **(A)** RT-qPCR reveals decreased expression of Par3 ( $n = 4$ ,  $P = 0.00058$ ), Pals1 ( $n = 4$ ,  $P = 0.0134$ ), Crumbs ( $n = 4$ ,  $P = 0.015$ ), and Scrib ( $n = 4$ ,  $P = 0.0081$ ) in *Klf4*<sup>Δ/ΔCE</sup> compared with the control corneas. **(B)** Immunoblots show decreased expression of Par3 ( $n = 4$ ,  $P = 0.039$ ), Pals1 ( $n = 4$ ,  $P = 0.034$ ), and Scrib ( $n = 4$ ,  $P = 0.003$ ) in *Klf4*<sup>Δ/ΔCE</sup> corneas compared with the control. For densitometric quantitation, actin staining intensity was used as a loading control. All data are presented as mean  $\pm$   $\frac{1}{2}$  SEM. **(C)** Immunofluorescent stain for Par3 (i–iii), Pals1 (iv–vi), Crumbs1 (vii–ix), and Scrib (x–xii) in the *Klf4*<sup>Δ/ΔCE</sup> corneas compared with the control. Corresponding no primary antibody controls are shown for each antibody ( $n = 4$ ; representative images shown). Please see Supplementary Figure S2 for higher magnification images.

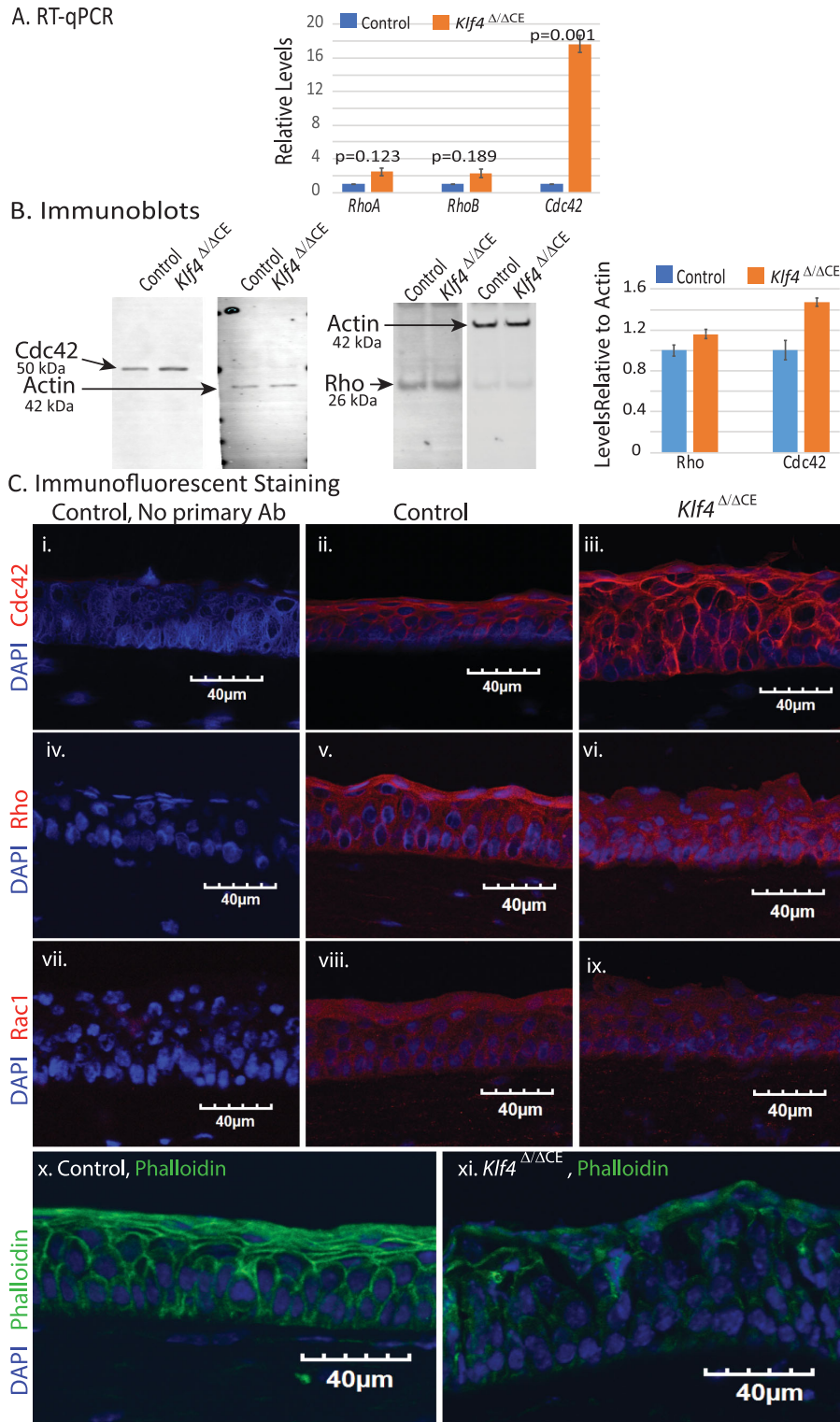


**FIGURE 2.** *Klf4*<sup>Δ/ΔCE</sup> cells display increased expression of Cdc42. (A) RT-qPCR revealed a modest increase in *RhoA* and *RhoB* transcripts in the *Klf4*<sup>Δ/ΔCE</sup> compared with the control corneas (*RhoA*:  $n = 4$ ,  $P = 0.123$  and *RhoB*:  $n = 4$ ,  $P = 0.189$ ) and a significant increase in *Cdc42* ( $n = 4$ ,  $P = 0.001$ ). (B) Immunoblots reveal increased expression of *Cdc42* ( $n = 4$ ,  $P = 0.016$ ) in the *Klf4*<sup>Δ/ΔCE</sup> corneas compared with the control. A similar increase was not observed in the Rho protein level ( $n = 4$ ,  $P = 0.495$ ). For densitometric quantitation, actin staining intensity was used as a loading control. All data are presented as mean  $\pm$   $\frac{1}{2}$  SEM. (C) Immunofluorescent stain shows increased expression of *Cdc42* (i–iii) in the *Klf4*<sup>Δ/ΔCE</sup> compared with the control CE. Rho (iv–vi) and Rac1 (vii–ix) are largely unaltered in the *Klf4*<sup>Δ/ΔCE</sup>. Staining with fluorescently tagged phalloidin (x–xi) revealed thick cortical F-actin bundles in control CE cells that were missing in the *Klf4*<sup>Δ/ΔCE</sup> cells. ( $n = 4$ ; representative images shown). Please see Supplementary Figure S3 for higher magnification images.

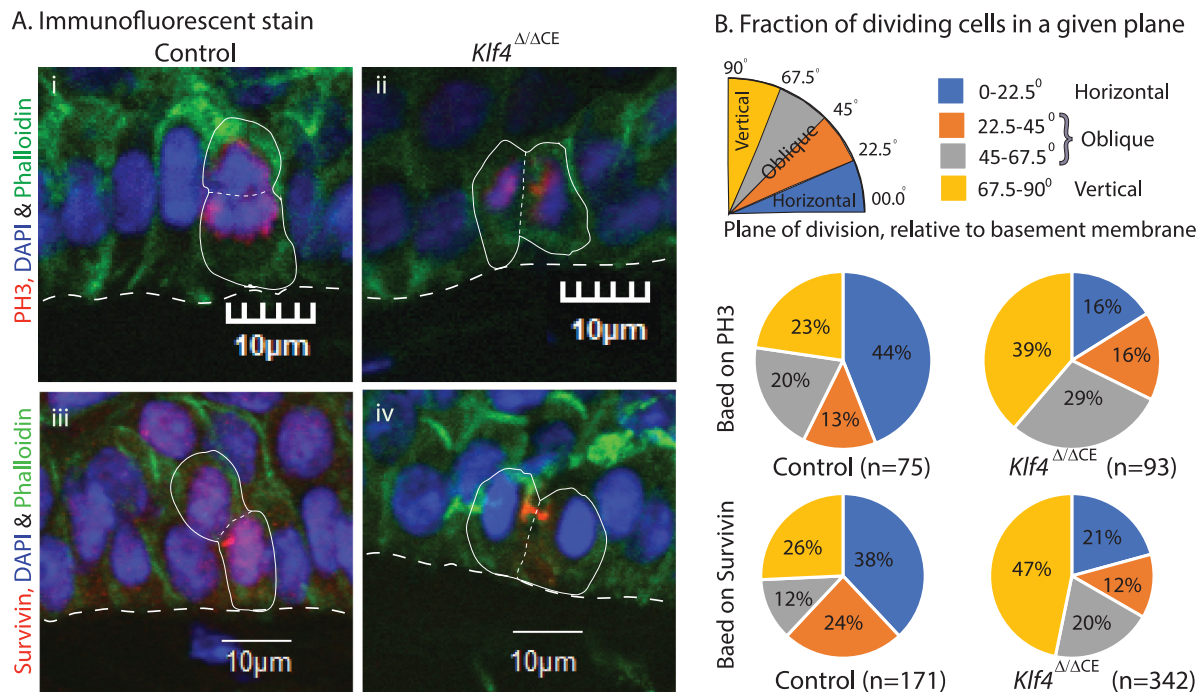


**FIGURE 3.** *Klf4*<sup>Δ/ΔCE</sup> CE cells favor vertical plane of division, unlike horizontal plane of division in the control CE. (A) Representative images of immunofluorescent stain with PH3 and antisurvivin antibodies in the control and *Klf4*<sup>Δ/ΔCE</sup> corneas. Basal CE cells stained for PH3 or survivin (red), F-actin (phalloidin; green), and nuclei (DAPI; blue) are shown with the plane of division marked by a thin dotted line relative to the basement membrane (dotted white line). Consistent with Figure 2, phalloidin stain intensity was lower in *Klf4*<sup>Δ/ΔCE</sup> corneal sections (panels ii and iv) compared with the control (panels i and iii). This intensity was selectively increased during postprocessing of the images presented here to facilitate detection of cellular boundaries. Thus, they appear even in this figure. (B) Distribution of the plane of division in control and *Klf4*<sup>Δ/ΔCE</sup> CE quantified by analyzing four adjacent images from the central CE in four sections each from five different eyeballs stained with anti-PH3 or antisurvivin antibody. Planes of division in the 0° to 22.5° range relative to CE basement membrane were considered horizontal, 22.5° to 67.5° range as oblique, and 67.5° to 90° range as vertical. Pie charts display the distribution of the plane of division relative to the basement membrane in the control and *Klf4*<sup>Δ/ΔCE</sup> CE. The number of nuclei counted in each condition (n value) and the percentage of cells falling in each group are indicated.

immunofluorescent stain revealed comparable expression of RhoA/B/C and Rac1 in the control and *Klf4*<sup>Δ/ΔCE</sup> corneas (Fig. 2C, Supplementary Fig. S3). Phalloidin stain revealed thick cortically localized F-actin cytoskeletal bundles in the control CE compared with those that were thin, lacked cortical localization, and were diffusely distributed in the *Klf4*<sup>Δ/ΔCE</sup> CE cytoplasm (Fig. 2C). Collectively, these results suggest that the loss of ABP in *Klf4*<sup>Δ/ΔCE</sup> CE cells is accompanied by overexpression of Cdc42 and disruption of the F-actin cytoskeletal network.

### Klf4 Promotes Horizontal Plane of Division in Basal CE Cells

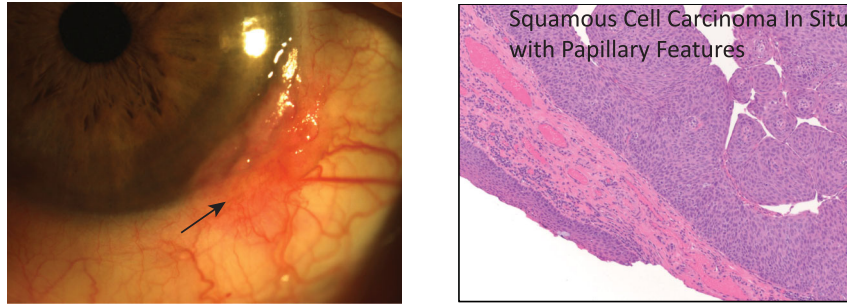
During cell division, mitotic spindle orientation and the plane of cell division are influenced by the cell's polarity, which in turn is regulated by the asymmetric enrichment of ABP complex proteins.<sup>36</sup> Given (1) the requirement for a proper balance between symmetric and asymmetric cell divisions during CE development and homeostasis,<sup>37</sup> (2) the influence of cellular polarity on plane of division,<sup>38</sup> (3) the dependence of stem cells on asymmetric cell division,<sup>39</sup> and (4) the role of Klf4 in maintenance of CE cell ABP described above, we next investigated if Klf4 is involved in regulating the CE plane of cell division. We evaluated the plane of cell division by immunofluorescent staining using PH3 and anti-

survivin antibodies (Fig. 3). A large fraction of the dividing cells in the control CE displayed a horizontal plane of division within 0° to 22.5° of the CE basement membrane (44% and 38%, relative to 16% and 21% in *Klf4*<sup>Δ/ΔCE</sup> CE based on PH3 and survivin, respectively). Such events with horizontal plane of division would presumably result in daughter cells with two different cell fates (i.e., proliferation and differentiation) essential for stratification.<sup>40</sup> In contrast, *Klf4*<sup>Δ/ΔCE</sup> CE favored vertical plane of cell division within 67.5° to 90° of the CE basement membrane (39% and 47% relative to 23% and 26% in the control CE based on PH3 and survivin, respectively), which is expected to produce the relatively increased number of dividing cells within *Klf4*<sup>Δ/ΔCE</sup> CE as reported earlier (Fig. 3).<sup>19</sup> No significant difference was observed in the number of cells undergoing oblique division within 22.5° to 67.5° of the basement membrane in control (33% and 36% based on PH3 and survivin staining, respectively) and *Klf4*<sup>Δ/ΔCE</sup> CE (45% and 32% with PH3 and survivin staining, respectively).

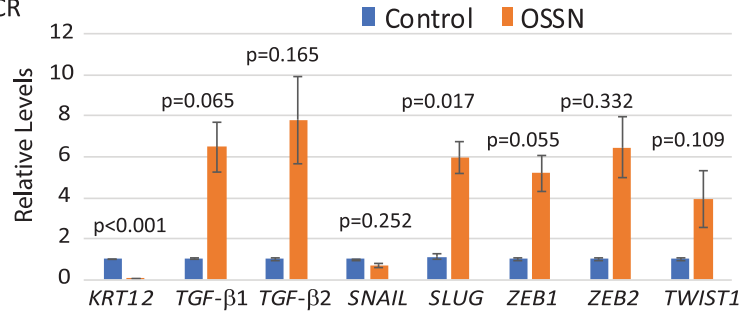
### EMT and Loss of ABP in Human OSSN Is Associated With Downregulation of KLF4

Previously, we reported that CE-specific ablation of *Klf4* results in defects that resemble OSSN.<sup>19,22,23</sup> To determine if OSSN is indeed accompanied by EMT, we obtained surgically

A. Clinical Presentation of OSSN and Histology



B. RT-qPCR



C. Immunofluorescent Stain, KRT12, Ki67 and Survivin

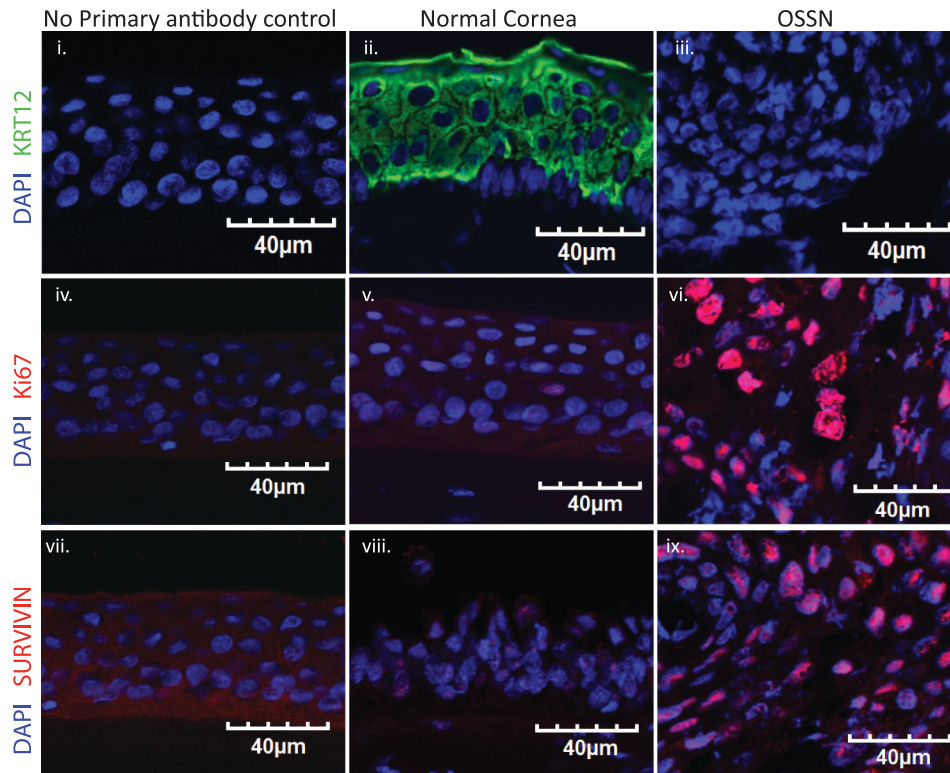


**FIGURE 4.** Signs of EMT in OSSN tissue. (A) En face image of OSSN and histology of excised tissue. Histology suggests squamous cell carcinoma in situ with papillary features. (B) RT-qPCR reveals downregulation of CE-specific marker KRT12 and upregulation of EMT inducers TGF-β1 and TGF-β2, as well as EMT transcription factors SLUG, ZEB1, ZEB2, and TWIST1 ( $n = 4$ ;  $P$  values shown). (C) Immunofluorescent stain reveals (i–iii) abundant expression of KRT12 (green) in (ii) normal CE but not (iii) OSSN and (iv–ix) abnormally high number of Ki67<sup>+</sup> and Survivin<sup>+</sup> cells in (red; vi and ix) OSSN relative to far fewer Ki67<sup>+</sup> and Survivin<sup>+</sup> cells in normal CE (red; v and viii). No primary antibody control for each antibody used is shown ( $n = 3$ ; representative images shown).

excised human tissues suspected of OSSN and ascertained OSSN by histology (Fig. 4A). RT-qPCR revealed significant downregulation of KRT12, a CE-specific marker and a KLF4-

target gene,<sup>16,18</sup> coupled with upregulation of EMT inducers TGF-β1 and TGF-β2, as well as EMT transcription factors SLUG, ZEB1, ZEB2, and TWIST1 in OSSN compared with the

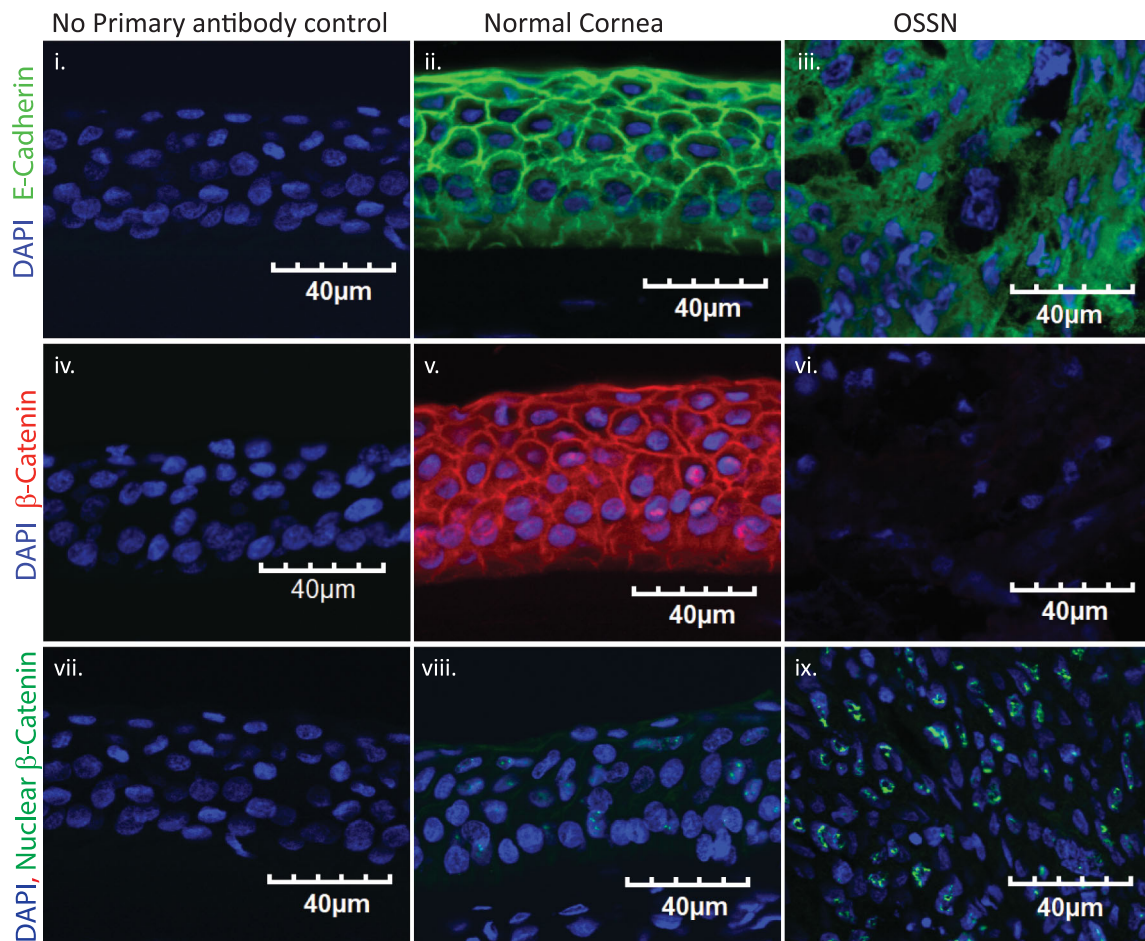


**FIGURE 5.** Loss of epithelial properties in OSSN. Immunofluorescent stain reveals abundant expression and proper membrane localization of (ii) E-cadherin and (v)  $\beta$ -catenin in the normal CE, compared with sharply decreased expression of (iii) E-cadherin that is diffusely localized in the cytoplasm and (vi)  $\beta$ -catenin in OSSN. Immunostaining with an antibody that specifically detects the nuclear  $\beta$ -catenin (green) revealed (ix) strong nuclear presence of  $\beta$ -catenin in many OSSN cells compared with a (viii) a faint expression in far fewer cells in the normal CE nuclei. No primary antibody control for each antibody used is shown ( $n = 3$ ; representative images shown).

normal CE (Fig. 4B, Supplementary Table S1). Immunofluorescent stain confirmed abundant expression of KRT12 in the normal CE, which was sharply decreased in OSSN tissues (Fig. 4C, Supplementary Table S1). Immunostaining also revealed an abnormally high frequency of Ki67<sup>+</sup> and survivin<sup>+</sup> cells in OSSN tissue compared with the normal control, consistent with the high rate of proliferation in OSSN tissues (Fig. 4C, Supplementary Table S1). Next, we confirmed the loss of epithelial features in OSSN tissues by evaluating the expression and localization of E-cadherin and  $\beta$ -catenin. Immunostaining revealed that both E-cadherin and  $\beta$ -catenin are abundantly expressed and properly localized to the cell membranes in the control CE, where they form a part of the adherens junctions (Fig. 5). In contrast, E-cadherin was diffusely localized in the cytoplasm and  $\beta$ -catenin was sharply downregulated and abnormally localized in nuclei, consistent with EMT in OSSN samples (Fig. 5, Supplementary Table S1).

Next, we determined if EMT in OSSN is also associated with a loss of ABP by testing the expression of PAR3, PALS1, and SCRIB. RT-qPCR revealed significant downregulation of *PAR3*, *PALS1*, and *SCRIB* in OSSN compared with the control CE (Fig. 6A, Supplementary Table S1). Consistently, immunostaining revealed that PAR3, PALS1, and SCRIB are

sharply downregulated in the OSSN cells compared with the control CE (Fig. 6B). Collectively, these data reveal that OSSN cells display different signs of EMT, including elevated cell proliferation, downregulation of epithelial markers, and loss of ABP determinants. Considering that each of these features was also observed in the *Klf4* <sup>$\Delta$ /CE</sup> corneas with CE-specific ablation of *Klf4*, we hypothesized that EMT and loss of ABP in OSSN is an outcome of downregulation of KLF4. Consistent with this prediction, RT-qPCR revealed significant downregulation of KLF4 in OSSN tissues, which was confirmed by immunofluorescent stain (Fig. 7, Supplementary Table S1). Collectively, these results demonstrate that KLF4 facilitates CE homeostasis by upregulating the expression of ABP complex components and promoting horizontal plane of division in dividing cells and that KLF4 is downregulated in OSSN tissues, which display signs of EMT and loss of ABP.

## DISCUSSION

Previously, we reported that CE-specific ablation of *Klf4* results in (1) EMT coupled with loss of CE barrier function and hyperplasia<sup>16,19,22</sup> and (2) activation of canonical TGF- $\beta$  signaling and downregulation of cell cycle inhibitors

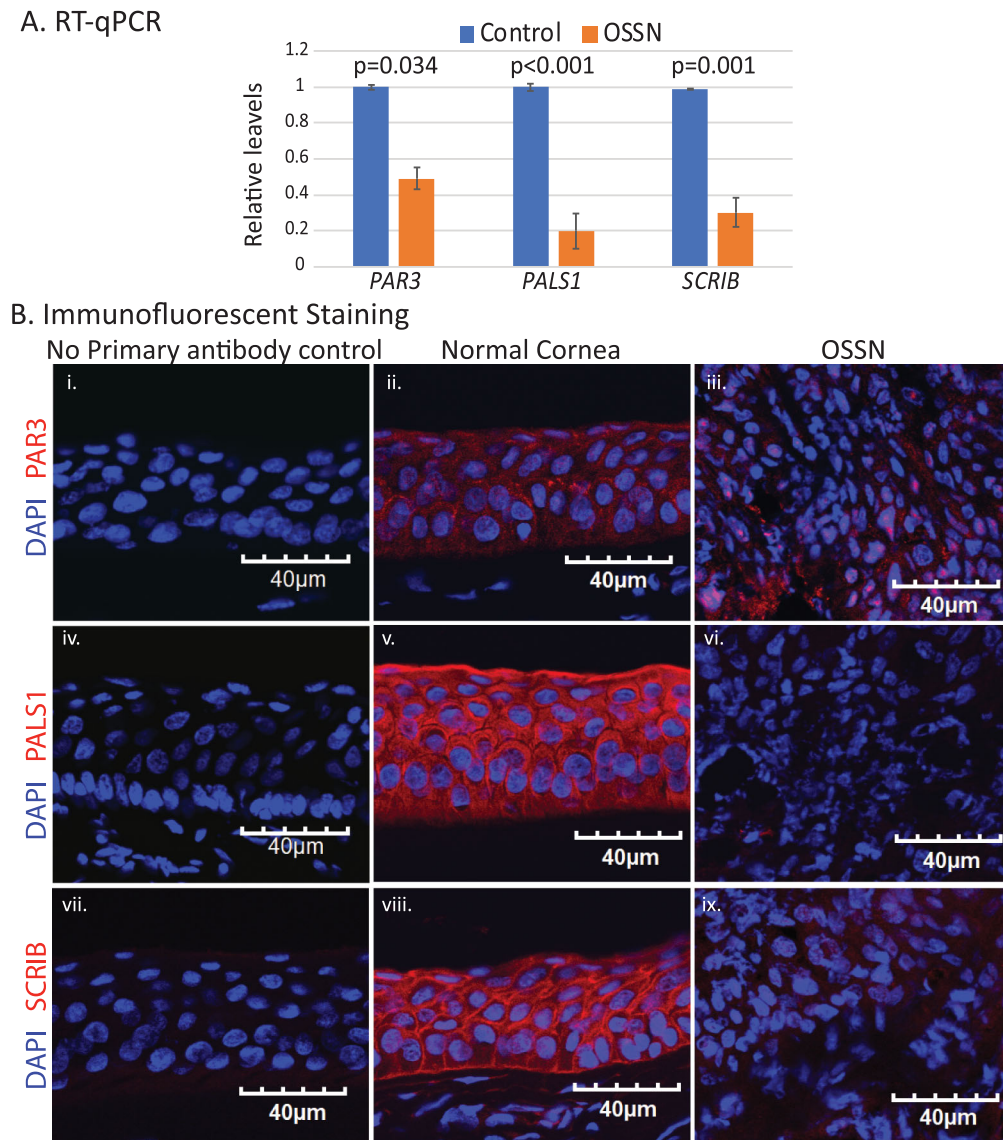


**FIGURE 6.** Loss of ABP in OSSN. **(A)** RT-qPCR reveals significant downregulation of *PAR3*, *PALS1*, and *SCRIB* transcripts in OSSN compared with the normal CE.  $n = 4$ ;  $P$  values shown on the graph. **(B)** Immunofluorescent staining reveals that the normal CE displays abundant expression and proper localization of (ii) *PAR3*, (v) *PALS1*, and (viii) *SCRIB*, which is sharply downregulated in the OSSN tissue (iii, vi, and ix, respectively). No primary antibody control for each antibody used is shown ( $n = 3$ ; representative images shown).

favoring increased proliferation.<sup>23</sup> The data presented in this report elucidate the crucial role of *Klf4* in orchestrating the CE stratification and homeostasis by coordinating the expression of a functionally related subset of determinants of ABP and plane of CE cell division (Fig. 8). Our data also demonstrate that (1) human OSSN tissues display signs of active EMT manifested as increased expression of TGF- $\beta$  and EMT transcription factors, (2) EMT in OSSN tissues is concurrent with loss of ABP, and (3) *Klf4* and its target genes *KRT12*, E-cadherin, and  $\beta$ -catenin are significantly downregulated in OSSN. Collectively, these results demonstrate that *Klf4* plays a key integrative role in coordinating CE cell polarity and plane of cell division and that the loss of this key function results in OSSN with potentially devastating consequences on sight (Fig. 8).

Unlike monolayered simple epithelial cells where ABP is defined by the attachment of the cells to the basement

membrane on the basal side, mechanisms that regulate the distribution of polarity-determining components across the stratified epithelial tissue are poorly understood.<sup>2</sup> Initial formation of a polarized stratified epithelium, as well as its homeostatic maintenance in the later adult stage, involves three crucial events: (1) establishment of ABP across different layers, (2) formation of apical tight junctions and apico-lateral adherence junctions, and (3) proper positioning of the mitotic spindle to enable asymmetric cell division.<sup>41</sup> CE-specific ablation of *Klf4* resulted in downregulation of tight and adherence junction proteins *Tjp1* and E-cadherin, respectively, suggesting a role for *Klf4* in regulating ABP.<sup>19,22</sup> Although the role of *Klf4* in regulating the expression of tight and adherence junction components is well defined,<sup>18,21</sup> its involvement in regulating ABP determinants *Crumbs*, *Pals1*, *Par3*, and *Scribble* was not described previously. Our observation that the loss of *Klf4* results in the loss of ABP provides

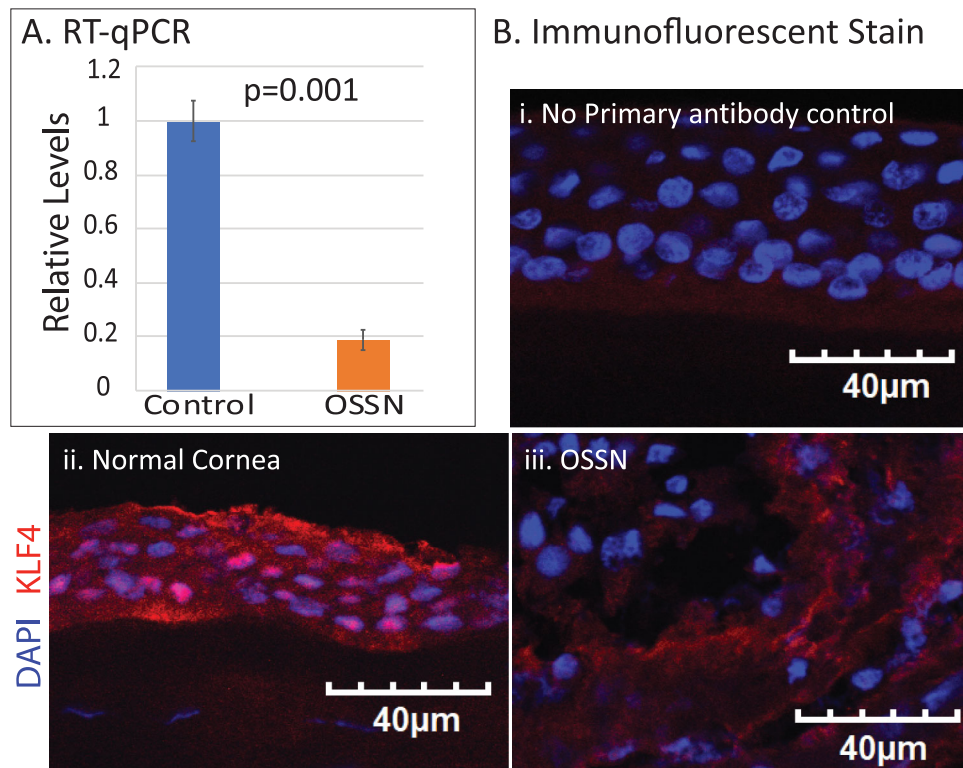


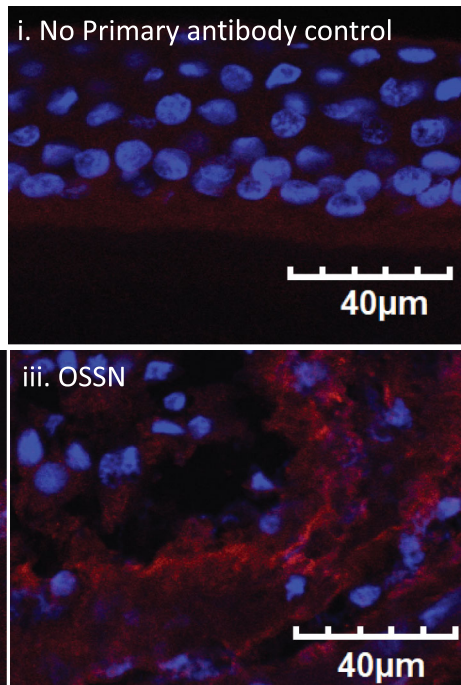
**FIGURE 7.** KLF4 is downregulated in OSSN. (A) RT-qPCR reveals significant downregulation of *KLF4* transcripts in OSSN compared with the normal CE ( $n = 4$ ;  $P$  values shown on the graph). (B) Immunofluorescent staining reveals that the normal CE displays abundant expression and proper nuclear localization of KLF4 (panel ii) that is sharply downregulated and mislocalized in the OSSN tissue (panel iii). No primary antibody control is shown (panel i) ( $n = 3$ ; representative images shown).

the first-ever evidence that *Klf4* plays a crucial role in maintaining the polarized nature of the stratified CE.

Although it is well established that different ABP complex components, including Crumbs, Par, and Scribble, are direct transcriptional targets of EMT inducers such as TGF- $\beta$ <sup>25,42</sup> and that the epithelial ABP is disrupted with the onset of EMT,<sup>43</sup> the underlying mechanistic basis for this disruption was not known. The CE-specific ablation of *Klf4* results in downregulation of epithelial genes and induction of EMT facilitated by robust TGF- $\beta$ -signaling.<sup>19,22,23</sup> Although the downregulation of ABP complex components in the *Klf4* <sup>$\Delta$ /CE</sup> CE described here suggests a supportive role for *Klf4* in maintaining ABP, whether this downregulation is a direct effect of the absence of *Klf4* or an indirect manifestation of the EMT mediated by upregulation of TGF- $\beta$  reported earlier<sup>22,23</sup> remains to be established.

Establishment and maintenance of cell polarity require efficient crosstalk between a complex network of different signaling pathways, including that involving Rho GTPase proteins.<sup>12,44,45</sup> Rho GTPases regulate cell shape and surface dynamics by orchestrating the communication between the cytoskeleton, contractile actin cortex, and the plasma membrane.<sup>45</sup> Among Rho GTPases, the expression of Cdc42, which contributes to the apical polarity by interacting with Par3<sup>46</sup> and regulates nucleation of actin filaments,<sup>47</sup> was upregulated in *Klf4* <sup>$\Delta$ /CE</sup> corneas, consistent with the ability of *Klf4* to inhibit Cdc42 expression via WNT5A.<sup>48</sup> Together, these results suggest that *Klf4* coordinates CE ABP by regulating the expression of Cdc42, which promotes nucleation and cortical arrangement of F-actin.<sup>13,35,45</sup>

## B. Immunofluorescent Stain



The data presented here demonstrate that CE-specific ablation of *Klf4* results in loss of ABP, which is essential for epithelial stratification and homeostasis. Asymmetric distribution of polarity determinants also governs the mitotic spindle orientation and promotes the asymmetric pattern of cell division, creating a pool of proliferating and differentiating cells aiding in the process of self-renewal in stratified tissues.<sup>40,44,49</sup> The current data elucidate that similar to other stratified tissues such as the epidermis,<sup>40</sup> the control CE displays more divisions with a horizontal plane that would presumably result in asymmetric divisions—a condition necessary for stratification. In contrast, the *Klf4* <sup>$\Delta$ /CE</sup> corneas displayed a tilt in the plane of division favoring vertical plane of division expected to result in daughter cells that retain the potential to further proliferate. Whether the CE ABP and the pattern of cell division progressively change from the corneal limbus to the central cornea, if there is a correlation between the two, and if *Klf4* has a role in coordinating them remain to be determined.

Previously, we demonstrated that the CE-specific ablation of *Klf4* results in EMT via elevated TGF- $\beta$  signaling.<sup>19,22,23</sup> The current report elucidates that *Klf4* ablation also results in the loss of ABP favoring vertical plane of division in the basal CE cells, which in turn creates a larger pool of proliferating cells. Collectively, these results suggest that *Klf4* contributes to CE stratification and homeostasis by promoting correct ABP and horizontal plane of division. Any imbalance favoring vertical plane of division as observed in the *Klf4* <sup>$\Delta$ /CE</sup> corneas is expected to result in excessive proliferation and compromised differentiation. Mutations and/or

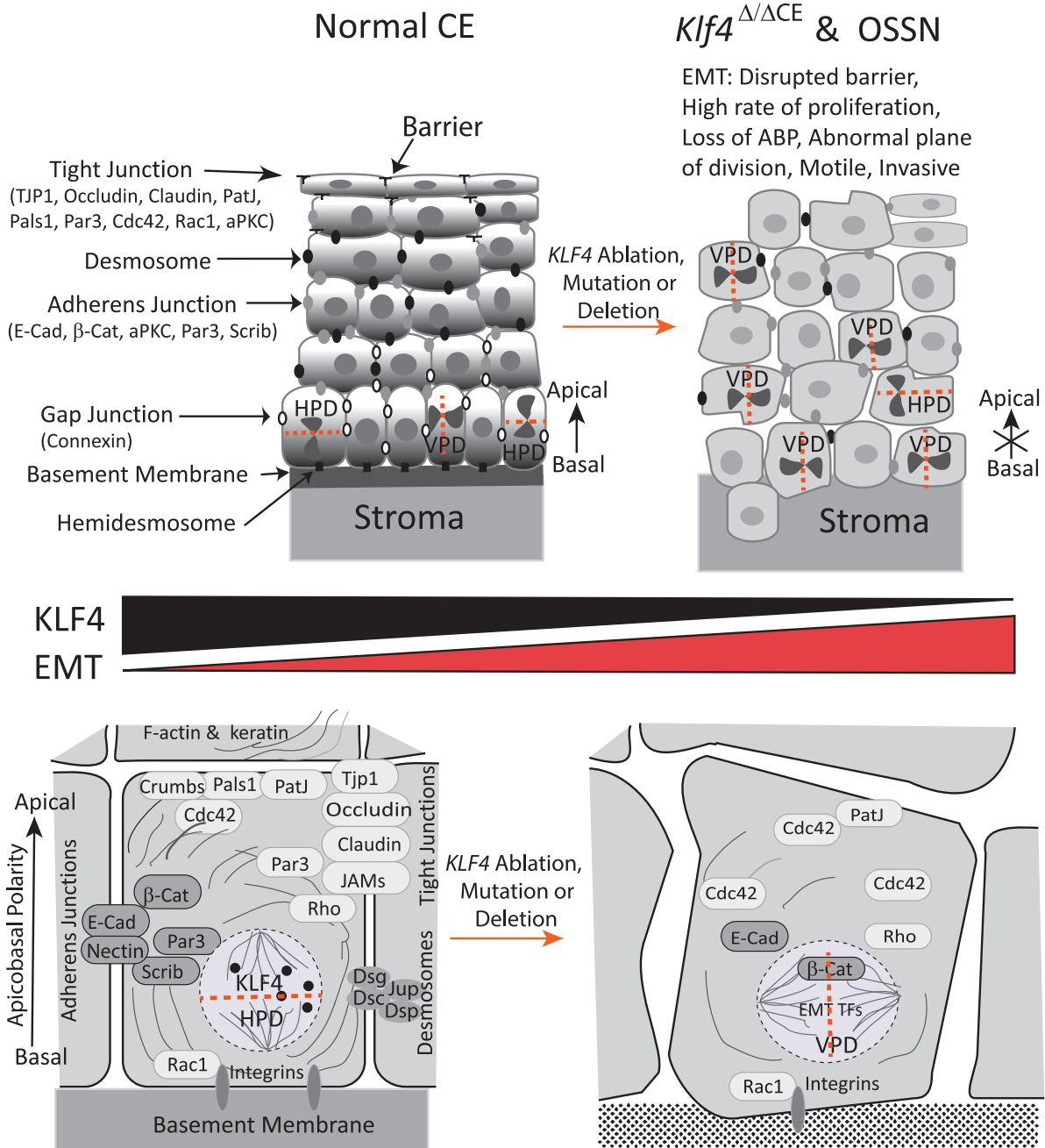


**FIGURE 8.** Schematic summarizing the findings described in this study. Mouse CE-specific ablation of *Klf4* resulted in disruption/downregulation of ABP core complex components and Cdc42 altering actin cytoskeletal organization and favoring the vertical plane of cell division (VPD) relative to the CE basement membrane compared with the horizontal plane of division (HPD) favored in the control. Downregulation of ABP core complex components in the human OSSN samples was coupled with decreased expression of KLF4. These changes are shown in greater detail in the lower panels. By demonstrating that *Klf4* ablation affects CE expression of ABP markers and Rho family GTPase Cdc42, cytoskeletal actin organization and the plane of cell division, and that KLF4 is downregulated in OSSN tissues that display EMT and lack ABP, these results elucidate the key integrative role of KLF4 in coordinating CE cell polarity and plane of division, the loss of which results in OSSN.

deletions in *KLF4* are associated with different tumors that also display EMT and excessive proliferation,<sup>27,50–52</sup> suggesting that KLF4 plays a protective role in the CE, the absence of which potentially drives the cells toward OSSN.<sup>53</sup> Consistent with this possibility, we observed unabated EMT and loss of ABP in human OSSN tissues that also displayed a sharp downregulation of *KLF4* expression.

In summary, our current findings reveal that KLF4 promotes CE stratification and homeostasis by regulating the proper expression of ABP core complex components and Cdc42, which in turn facilitate proper arrangement of the mitotic spindle favoring horizontal plane of cell division. By demonstrating that *Klf4* ablation affects CE expression of ABP markers and Rho family GTPases, cytoskeletal actin

organization, and the plane of cell division and that KLF4 is downregulated in OSSN tissues that lack ABP and display EMT, these results elucidate the key integrative role of KLF4 in coordinating CE cell polarity and plane of division, the loss of which results in OSSN (Fig. 8).

### Acknowledgments

The authors thank John Gnalian for technical help, Kate Davoli (Tissue Culture and Histology Core Module) for help with histology, Kira Lathrop (Imaging Core Module) for help with imaging, Xiangyun Wei for the generous gift of Crumbs1 antibody, and Debasish Sinha for critical comments on the manuscript.

Supported by NIH Grant R01 EY026533 (SKS) and NEI core Grant P30 EY08098, as well as by unrestricted grants from Research to Prevent Blindness and the Eye and Ear Foundation of Pittsburgh. The authors alone are responsible for the content and writing of the paper.

Disclosure: **A. Tiwari**, None; **S. Swamynathan**, None; **V. Jhanji**, None; **S.K. Swamynathan**, None

### References

- Swamynathan SK. Ocular surface development and gene expression. *J Ophthalmol*. 2013;2013:103947.
- Niessen MT, Iden S, Niessen CM. The in vivo function of mammalian cell and tissue polarity regulators—how to shape and maintain the epidermal barrier. *J Cell Sci*. 2012;125:3501–3510.
- Rodriguez-Boulan E, Macara IG. Organization and execution of the epithelial polarity programme. *Nat Rev Mol Cell Biol*. 2014;15:225–242.
- Vasioukhin V, Bauer C, Degenstein L, Wise B, Fuchs E. Hyperproliferation and defects in epithelial polarity upon conditional ablation of alpha-catenin in skin. *Cell*. 2001;104:605–617.
- Thoft RA, Friend J. The X, Y, Z hypothesis of corneal epithelial maintenance. *Invest Ophthalmol Vis Sci*. 1983;24:1442–1443.
- Cutler TJ. Corneal epithelial disease. *Vet Clin North Am Equine Pract*. 2004;20:319–343, vi.
- Findlay AS, Panzica DA, Walczysko P, et al. The core planar cell polarity gene, Vangl2, directs adult corneal epithelial cell alignment and migration. *R Soc Open Sci*. 2016;3:160658.
- Panzica DA, Findlay AS, van Ladesteijn R, Collinson JM. The core planar cell polarity gene, Vangl2, maintains apical-basal organisation of the corneal epithelium. *J Anat*. 2019;234:106–119.
- Assemat E, Bazellieres E, Pallesi-Pocachard E, Le Bivic A, Massey-Harroche D. Polarity complex proteins. *Biochim Biophys Acta*. 2008;1778:614–630.
- Wang Q, Hurd TW, Margolis B. Tight junction protein Par6 interacts with an evolutionarily conserved region in the amino terminus of PALS1/stardust. *J Biol Chem*. 2004;279:30715–30721.
- Roh MH, Fan S, Liu CJ, Margolis B. The Crumbs3-Pals1 complex participates in the establishment of polarity in mammalian epithelial cells. *J Cell Sci*. 2003;116:2895–2906.
- Iden S, Collard JG. Crosstalk between small GTPases and polarity proteins in cell polarization. *Nat Rev Mol Cell Biol*. 2008;9:846–859.
- Sit ST, Manser E. Rho GTPases and their role in organizing the actin cytoskeleton. *J Cell Sci*. 2011;124:679–683.
- Conboy IM, Rando TA. The regulation of Notch signaling controls satellite cell activation and cell fate determination in postnatal myogenesis. *Dev Cell*. 2002;3:397–409.
- Kuang S, Kuroda K, Le Grand F, Rudnicki MA. Asymmetric self-renewal and commitment of satellite stem cells in muscle. *Cell*. 2007;129:999–1010.
- Swamynathan SK, Katz JP, Kaestner KH, Ashery-Padan R, Crawford MA, Piatigorsky J. Conditional deletion of the mouse Klf4 gene results in corneal epithelial fragility, stromal edema, and loss of conjunctival goblet cells. *Mol Cell Biol*. 2007;27:182–194.
- Stephens DN, Klein RH, Salmans ML, Gordon W, Ho H, Andersen B. The Ets transcription factor EHF as a regulator of cornea epithelial cell identity. *J Biol Chem*. 2013;288:34304–34324.
- Swamynathan SK, Davis J, Piatigorsky J. Identification of candidate Klf4 target genes reveals the molecular basis of the diverse regulatory roles of Klf4 in the mouse cornea. *Invest Ophthalmol Vis Sci*. 2008;49:3360–3370.
- Delp EE, Swamynathan S, Kao WW, Swamynathan SK. Spatiotemporally regulated ablation of Klf4 in adult mouse corneal epithelial cells results in altered epithelial cell identity and disrupted homeostasis. *Invest Ophthalmol Vis Sci*. 2015;56:3549–3558.
- Yori JL, Johnson E, Zhou G, Jain MK, Keri RA. Kruppel-like factor 4 inhibits epithelial-to-mesenchymal transition through regulation of E-cadherin gene expression. *J Biol Chem*. 2010;285:16854–16863.
- Swamynathan S, Kenchegowda D, Piatigorsky J, Swamynathan SK. Regulation of corneal epithelial barrier function by Kruppel-like transcription factor 4. *Invest Ophthalmol Vis Sci*. 2011;52:1762–1769.
- Tiwari A, Loughner CL, Swamynathan S, Swamynathan SK. KLF4 plays an essential role in corneal epithelial homeostasis by promoting epithelial cell fate and suppressing epithelial-mesenchymal transition. *Invest Ophthalmol Vis Sci*. 2017;58:2785–2795.
- Tiwari A, Swamynathan S, Alexander N, et al. KLF4 regulates corneal epithelial cell cycle progression by suppressing canonical TGF-beta signaling and upregulating CDK inhibitors P16 and P27. *Invest Ophthalmol Vis Sci*. 2019;60:731–740.
- Yu T, Chen X, Zhang W, et al. Kruppel-like factor 4 regulates intestinal epithelial cell morphology and polarity. *PLoS One*. 2012;7:e32492.
- Wang X, Nie J, Zhou Q, et al. Downregulation of Par-3 expression and disruption of Par complex integrity by TGF-beta during the process of epithelial to mesenchymal transition in rat proximal epithelial cells. *Biochim Biophys Acta*. 2008;1782:51–59.
- Yu M, Hao B, Zhan Y, Luo G. Kruppel-like factor 4 expression in solid tumor prognosis: a meta-analysis. *Clin Chim Acta*. 2018;485:50–59.
- Ghaleb AM, Yang, Kruppel-like VW. factor 4 (KLF4): what we currently know. *Gene*. 2017;611:27–37.
- Halaoui R, McCaffrey L. Rewiring cell polarity signaling in cancer. *Oncogene*. 2015;34:939–950.
- Katz JP, Perreault N, Goldstein BG, et al. The zinc-finger transcription factor Klf4 is required for terminal differentiation of goblet cells in the colon. *Development*. 2002;129:2619–2628.
- Chikama T, Hayashi Y, Liu CY, et al. Characterization of tetracycline-inducible bitransgenic Krt12rtTA+/tet-O-LacZ mice. *Invest Ophthalmol Vis Sci*. 2005;46:1966–1972.
- Hayashi Y, Call MK, Liu CY, et al. Monoallelic expression of Krt12 gene during corneal-type epithelium differentiation of limbal stem cells. *Invest Ophthalmol Vis Sci*. 2010;51:4562–4568.
- Iden S, van Riel WE, Schafer R, et al. Tumor type-dependent function of the par3 polarity protein in skin tumorigenesis. *Cancer Cell*. 2012;22:389–403.
- McCaffrey LM, Macara IG. Signaling pathways in cell polarity. *Cold Spring Harb Perspect Biol*. 2012;4:a009654.

34. Bray K, Gillette M, Young J, et al. Cdc42 overexpression induces hyperbranching in the developing mammary gland by enhancing cell migration. *Breast Cancer Res.* 2013;15:R91.
35. Mack NA, Georgiou M. The interdependence of the Rho GTPases and apicobasal cell polarity. *Small GTPases.* 2014;5:10.
36. Wen W, Zhang M. Protein complex assemblies in epithelial cell polarity and asymmetric cell division. *J Mol Biol.* 2018;430:3504–3520.
37. Castro-Munozledo F, Gomez-Flores E. Challenges to the study of asymmetric cell division in corneal and limbal epithelia. *Exp Eye Res.* 2011;92:4–9.
38. Campanale JP, Sun TY, Montell DJ. Development and dynamics of cell polarity at a glance. *J Cell Sci.* 2017;130:1201–1207.
39. Jiang J, Chan YS, Loh YH, et al. A core Klf circuitry regulates self-renewal of embryonic stem cells. *Nat Cell Biol.* 2008;10:353–360.
40. Lechler T, Fuchs E. Asymmetric cell divisions promote stratification and differentiation of mammalian skin. *Nature.* 2005;437:275–280.
41. McCaffrey LM, Macara IG. organization, cell polarity and tumorigenesis. *Trends Cell Biol.* 2011;21:727–735.
42. Aigner K, Dampier B, Descovich L, et al. The transcription factor ZEB1 (deltaEF1) promotes tumour cell dedifferentiation by repressing master regulators of epithelial polarity. *Oncogene.* 2007;26:6979–6988.
43. Moreno-Bueno G, Portillo F, Cano A. Transcriptional regulation of cell polarity in EMT and cancer. *Oncogene.* 2008;27:6958–6969.
44. Nelson WJ. Adaptation of core mechanisms to generate cell polarity. *Nature.* 2003;422:766–774.
45. de Curtis I, Meldolesi J. Cell surface dynamics—how Rho GTPases orchestrate the interplay between the plasma membrane and the cortical cytoskeleton. *J Cell Sci.* 2012;125:4435–4444.
46. Joberty G, Petersen C, Gao L, Macara IG. The cell-polarity protein Par6 links Par3 and atypical protein kinase C to Cdc42. *Nat Cell Biol.* 2000;2:531–539.
47. Ho HY, Rohatgi R, Lebensohn AM, et al. Toca-1 mediates Cdc42-dependent actin nucleation by activating the N-WASP-WIP complex. *Cell.* 2004;118:203–216.
48. Tetreault MP, Weinblatt D, Shaverdashvili K, Yang Y, Katz JP. KLF4 transcriptionally activates non-canonical WNT5A to control epithelial stratification. *Sci Rep.* 2016;6:26130.
49. Johnston D, Ahringer J. Cell polarity in eggs and epithelia: parallels and diversity. *Cell.* 2010;141:757–774.
50. Tang H, Zhu H, Wang X, et al. KLF4 is a tumor suppressor in anaplastic meningioma stem-like cells and human meningiomas. *J Mol Cell Biol.* 2017;9:315–324.
51. Rowland BD, Peeper DS. KLF4, p21 and context-dependent opposing forces in cancer. *Nat Rev Cancer.* 2006;6:11–23.
52. Park CS, Lewis A, Chen T, Lacorazza D. Concise review: regulation of self-renewal in normal and malignant hematopoietic stem cells by Kruppel-like factor 4. *Stem Cells Transl Med.* 2019;8:568–574.
53. Sudesh S, Rapuano CJ, Cohen EJ, Eagle RC, Jr, Laibson PR. Surgical management of ocular surface squamous neoplasms: the experience from a cornea center. *Cornea.* 2000;19:278–283.